https://doi.org/10.5194/egusphere-2025-204
Preprint. Discussion started: 21 February 2025

Subglacial hydrology regulates oscillations in marine ice streams

Marianne Haseloff[1], Ian J. Hewitt[2], and Richard F. Katz[3]

[1]Department of Geoscience, University of Wisconsin-Madison, Madison, WI 53706, USA
[2]Mathematical Institute, University of Oxford, Oxford OX2 6GG, UK
[3]Department of Earth Sciences, University of Oxford, Oxford OX1 3QR, UK

Correspondence: Marianne Haseloff (mhaseloff@wisc.edu)

Abstract. Marine ice stream dynamics are sensitive to conditions at the grounding line and basal shear stress; variations in subglacial hydrology have been implicated in ice stream speed-up and shutdown. To investigate the interplay between marine ice stream flow and subglacial hydrology, we couple models of a marine ice stream and a subglacial drainage system. The coupled system evolves dynamically due to a positive feedback between ice flow, heat dissipation at the ice stream bed, and basal lubrication. Our results show that depending on the hydraulic conductivity of the bed, distinct dynamic regimes can be identified. These regimes include steady streaming, hydraulically controlled surges, and thermally controlled oscillations. Periodic fast flow can be initiated by activation waves travelling upstream or downstream or quasi-simultaneously everywhere. Different dynamical regimes are characterised by large differences in grounded ice volume, even under modest changes of grounding line positions. These results imply a strong dependence of marine ice-sheet dynamics on evolving hydrological conditions at the bed and highlight the importance of a better understanding of subglacial hydrology.

1 Introduction

Much of the West Antarctic Ice Sheet rests on a bed that is below sea level, making it a marine ice sheet. Most of its mass is discharged by regions of fast flow with velocities in excess of 100 m yr^{-1} (called ice streams) embedded in regions of slow flow with velocities of only a few meters per year (Rignot et al., 2011). While most of West Antarctica has experienced dramatic mass loss in the last four decades, the Siple Coast region has a net positive mass balance (Rignot et al., 2019, 2022). This is due to the current inactivity of Kamb ice stream, which slowed down approximately 130 years ago (Retzlaff and Bentley, 1993) and the ongoing slow down of Whillans, Mercer, and MacAyeal ice streams (Stephenson and Bindschadler, 1988; Bindschadler and Vornberger, 1998; Joughin et al., 2002; Rignot et al., 2022). On longer time-scales, observations suggest that marine ice stream flow speeds vary on time scales of hundreds to thousands of years and can undergo shut-down-and-reactivation cycles (Hulbe and Fahnestock, 2007; Catania et al., 2012). Our aim in this paper is to better understand what role subglacial hydrology plays in these processes.

Some studies have suggested that subglacial hydrology is responsible for the speed up and slow down of Antarctic ice streams (Anandakrishnan and Alley, 1997; Elsworth and Suckale, 2016). Observations support the existence of a dynamic subglacial drainage system beneath West Antarctica's ice streams (Engelhardt and Kamb, 1997; Fricker et al., 2007). However, existing observational work does not address the interplay between subglacial hydrology and marine ice sheet dynamics.

https://doi.org/10.5194/egusphere-2025-204
Preprint. Discussion started: 21 February 2025

Conversely, theoretical studies of marine ice sheet dynamics usually focus on static basal boundary conditions (e.g., Weertman, 1974; Schoof, 2007a, b, 2012; Tsai et al., 2015; Joughin et al., 2019; Sergienko and Wingham, 2019; Sergienko and Haseloff, 2023) or prescribe their evolution (Brondex et al., 2017; Sergienko and Wingham, 2024). These studies show that the dynamics of the grounding line, which delineates the transition between grounded and floating ice, are sensitive to the basal boundary conditions. However, without an evolving subglacial drainage system, these models do not investigate which dynamic feedbacks exist between marine ice-stream dynamics and subglacial drainage.

Investigation of the interaction between ice-stream flow and subglacial drainage raises the question of how regions of fast and slow flow can co-exist in close proximity. One answer to this question invokes a positive feedback between heat dissipation and ice flow. Different mechanisms for this feedback have been hypothesised, relating it to either viscous weakening or to basal heat dissipation (e.g., Clarke et al., 1977; Fowler and Johnson, 1996; Payne and Dongelmans, 1997; Bougamont et al., 2011; Robel et al., 2014; Kyrke-Smith et al., 2014, 2015; Brinkerhoff and Johnson, 2015; Schoof and Mantelli, 2021). In this study, we focus on the latter feedback.

If the basal temperature is at the melting point, rapid sliding is possible and heat dissipation can be focused at the bed. The dominant positive feedback mechanism then involves melting at the base of the ice; faster sliding leads to more heat dissipation, which in turn produces additional melt water that reduces basal drag and permits even faster sliding. For this positive feedback to operate, melt water production must raise the water pressure at the bed, and hence reduce the effective pressure, defined as the difference between ice overburden and basal water pressure. This behaviour can be caused by two mechanisms. In the first, the effective pressure decreases through an increase in water storage at the bed. If water storage is in subglacial till and no drainage is possible, this is called the undrained bed model (e.g., Tulaczyk et al., 2000b; Sayag and Tziperman, 2008). In the second, an increase in discharge reduces the effective pressure (as is common for distributed hydrologic systems, e.g., Fowler and Johnson, 1996; Kyrke-Smith et al., 2014).

Several studies using the undrained bed model have shown that the positive feedback between fast flow and lubrication can explain oscillatory behaviour of ice streams when modulated by a thermodynamic feedback (MacAyeal, 1993; Fowler and Johnson, 1996; Payne and Dongelmans, 1997; Fowler and Schiavi, 1998; Bougamont et al., 2003; Christoffersen and Tulaczyk, 2003; Robel et al., 2013, 2014; Feldmann and Levermann, 2017). Faster ice flow results in dynamic thinning. When the ice thickness becomes too small, the amount of conductive cooling at the bed exceeds the heat dissipation due to flow and the ice stream shuts down. However, these studies neglect the transport of water and its effect on water content of the bed.

Fewer theoretical studies investigate the role of the second process (i.e., of subglacial hydrology), and these studies do not account for the subglacial conditions at the grounding line (Fowler and Johnson, 1996; Kyrke-Smith et al., 2014). Nevertheless, large-scale models capable of including these dynamics are beginning to emerge (e.g., Kazmierczak et al., 2022, 2024), motivating a better understanding of these processes. An extreme example of a subglacial drainage model assumes that subglacial hydrology is so efficient that hydraulic gradients cannot develop. Steady grounding lines are possible in this case (Tsai et al., 2015).

The goal of this study is to investigate the simplest possible feedback between fast flow, heat dissipation, and basal lubrication, and its role in marine ice sheet dynamics. We use a model that includes the positive feedback between fast flow and

https://doi.org/10.5194/egusphere-2025-204
Preprint. Discussion started: 21 February 2025

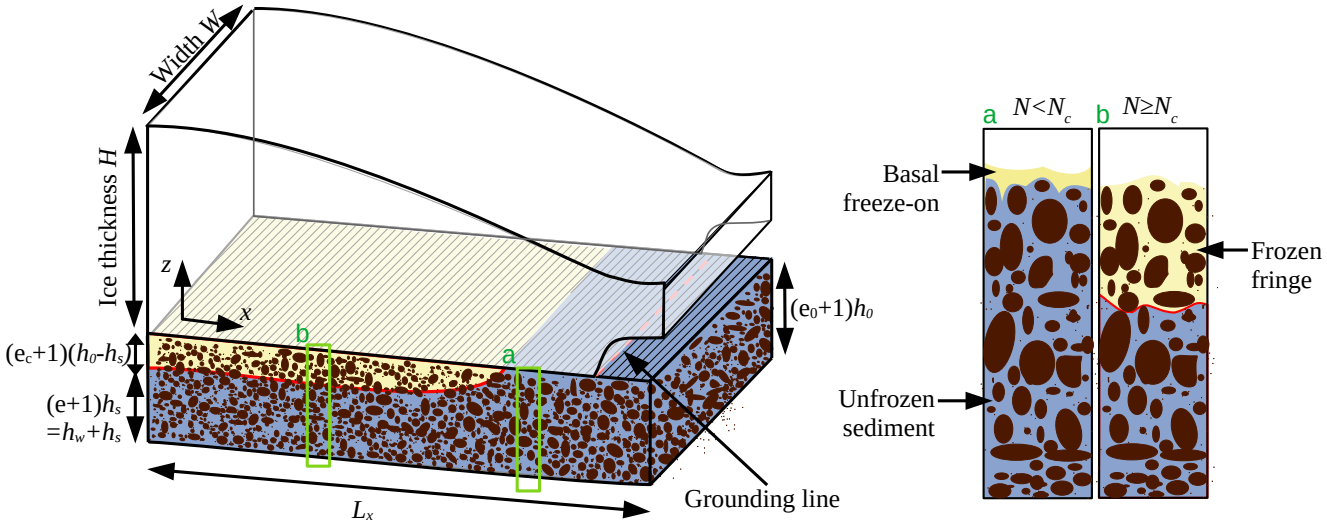

Figure 1. Model geometry and details of freezing. A marine ice sheet of thickness H and width W flows on a downwards sloping bed, becoming afloat at the grounding line. The underlying sediment is of thickness $(\mathrm{e}+1)h_s + (\mathrm{e}_c+1)(h_0-h_s)$ with e the void ratio of the unfrozen sediment, e_c the void ratio at which the sediment freezes, h_0 the thickness of the sediment layer if all void space was removed from it (i.e., at $\mathrm{e}=0$), and $(\mathrm{e}+1)h_s$ the thickness of the expanded, hydraulically active, unfrozen portion of the sediment. At effective pressures N below the critical effective pressure N_c, freezing is focused at the ice–bed contact (panel a). At $N \geq N_c$, freezing can intrude into the void space between sediment grains, and a frozen fringe forms (panel b).

basal lubrication through both storage of water in the subglacial sediment as well as evacuation of water through an active subglacial drainage system. The balance of these two processes is determined by the hydraulic conductivity of the bed. At very low hydraulic conductivity, the model reproduces the undrained bed model, and water content of the bed is determined by the local energy balance. At very high hydraulic conductivities, hydraulic gradients cannot develop at the bed; in this limit the effective pressure at the bed is set by the ice and bed geometry alone, independent of the local melt rate.

The main novelty of our study is the investigation of marine ice sheet dynamics over the entire spectrum of different hydraulic conductivities of the subglacial system. This puts the results of existing studies with vanishing (Robel et al., 2014) and infinite (Tsai et al., 2015) hydraulic conductivities into context. We find that at finite hydraulic conductivities of the bed, the interplay between local water storage and subglacial drainage can lead to oscillations with distinct character and frequency. These hydraulically induced dynamics differ from those previously reported (MacAyeal, 1993; Robel et al., 2014); they are controlled by the efficiency of the subglacial drainage system, rather than the local melt rate at the bed.

https://doi.org/10.5194/egusphere-2025-204
Preprint. Discussion started: 21 February 2025

2 The Model

We formulate the simplest possible model with an evolving hydraulic system and grounding line dynamics. Naturally, such a model must parameterize or neglect some other important aspects of ice-sheet dynamics and we discuss the limitations of our model below in section 4.4.

The computational domain is a flow line of length $L_x = 1000$ km with a downward sloping bed at elevation $b = z_0 - z_1 x$. All parameters are listed in table 1. We solve for velocity u, ice thickness H, water content of the bed h_w, and thickness of unexpanded, hydraulically active till layer h_s, which can evolve due to freezing and melting in the sediment, see figure 1.

2.1 Ice mechanics

We use a standard, depth- and width-integrated flowline model for ice sheet dynamics (Dupont and Alley, 2005; Nick et al., 2009; Robel et al., 2014; Haseloff and Sergienko, 2018). The ice thickness H evolves according to the equation for mass balance,

$$\frac{\partial H}{\partial t} + \frac{\partial (Hu)}{\partial x} = a, \tag{1}$$

with u the ice velocity in the downstream x–direction, and a the surface mass balance term (positive for net accumulation). The velocity u is determined from stress balance (e.g., MacAyeal, 1989; Hindmarsh, 2012; Pegler, 2016),

$$2\frac{\partial}{\partial x}\left[A^{-1/n} H \left[\left|\frac{\partial u}{\partial x}\right|^2 + \varepsilon^2\right]^{\frac{1-n}{2n}} \frac{\partial u}{\partial x}\right] - \tau_b - \frac{C_w A^{-1/n}}{W^{1/n+1}} H |u|^{1/n} \frac{u}{|u|} = \rho_i g H \frac{\partial (H+b)}{\partial x}, \tag{2}$$

with A the rate factor, n a rheological parameter, ε a parameter that regularises regions with zero strain rates, and τ_b the basal shear stress. The third term parameterises the lateral shear stress with the width of the outlet glacier W; C_w is a constant.

In accordance with recent studies, we assume that the relationship between basal shear stress τ_b and velocity u is of a regularized-Coulomb form (Zoet and Iverson, 2020). For large velocities, the basal shear stress becomes independent of the velocity and only depends on the effective pressure $N = \rho_i g H - p_w$, the difference between ice overburden and water pressure. We use a regularized version of the slip law used in Tsai et al. (2015),

$$\tau_b = \frac{C|u|^m \mu N}{C|u|^m + \mu N} \frac{u}{|u|}. \tag{3}$$

For $\mu N \gg C|u|^m$ this reproduces a Weertman-style sliding law $\tau_b \sim C|u|^m$, while for $\mu N \ll C|u|^m$ this mimics the Coulomb-plastic rheology $\tau_b \sim \mu N$ expected to be applicable to West Antarctic subglacial tills (Zoet and Iverson, 2020).

We are interested in interactions of the subglacial drainage system with ice-stream flow, which are coupled through the effective pressure N. Modelling the evolution of N requires a theory for the evolution of the subglacial drainage system. We turn to this next.

https://doi.org/10.5194/egusphere-2025-204
Preprint. Discussion started: 21 February 2025

Name	Symbol	Value	Units
Rate factor	A	1.6×10^{-24}	$\mathrm{Pa}^{-3}\ \mathrm{s}^{-1}$
Accumulation	a	0.3	$\mathrm{m\ yr}^{-1}$
Sliding parameter	C	15.8×10^{6}	$\mathrm{Pa\ (m\ s}^{-1})^{-1/3}$
Coefficient of compressibility	C_e	0.0345	
Lateral drag parameter	C_w	$2(n+1)^{1/n}$	
Void ratio at freezing	e_c	0.5178	
Void ratio corresponding to $N = 0$	e_0	1	
Void ratio reference parameter	e_r	0.78	
Gravitational acceleration	g	9.81	$\mathrm{m\ s}^{-2}$
Drained hydraulically active sediment thickness	h_0	1	m
Thermal conductivity	k	2	$\mathrm{W\ m}^{-1}\ \mathrm{K}^{-1}$
Hydraulic conductivity of the bed	K_d		$\mathrm{m\ s}^{-1}$
Latent heat	L_h	330×10^{3}	$\mathrm{J\ kg}^{-1}$
Domain length	L_x	10^{6}	m
Sliding parameter	m	$1/n$	
Sliding parameter	μ	0.5	
Viscosity parameter	n	3	
Critical effective pressure for freezing	N_c	2×10^{6}	Pa
Reference value of effective pressure	N_r	10^{3}	Pa
Geothermal heat flux	q_{geo}	65×10^{-3}	$\mathrm{W\ m}^{-2}$
Density of ice	ρ_i	910	$\mathrm{kg\ m}^{-3}$
Density of water	ρ_w	10^{3}	$\mathrm{kg\ m}^{-3}$
Melting point temperature	T_m	273	K
Surface temperature	T_s	$-20 + T_m$	K
Ice stream width	W	50	km
Bed offset	z_0	100	m
Bed slope	z_1	10^{-3}	

Table 1. Model parameters and their values.

2.2 Subglacial drainage

Many models describing subglacial drainage exist (Flowers, 2015). All models share the assumption that water is conserved at the bed and flows in the direction of hydraulic gradients (Flowers, 2015). However, only few models are applicable to softbedded glaciers (Walder and Fowler, 1994; Ng, 2000). We write conservation of water mass as (Clarke, 2005; Flowers,

https://doi.org/10.5194/egusphere-2025-204
Preprint. Discussion started: 21 February 2025

2015)

$$\frac{\partial h_w}{\partial t} + \frac{\partial q_w}{\partial x} = m_b, \tag{4}$$

where h_w is the effective water depth at the bed, q_w is the water flux, and m_b is the basal melt rate.

We assume that the hydraulic conductivity depends on the water content of the bed, as is common for distributed systems (Hewitt, 2011). This can also be modified to capture the formation of subglacial conduits (Sommers et al., 2018). However, aiming to keep our model as simple as possible, we write for the water flux

$$q_w = -\frac{K_{d,\text{eff}} h_s}{\rho_w g} \frac{\partial \Phi}{\partial x} \qquad \text{with} \qquad K_{d,\text{eff}} = K_d \frac{N_c}{N}. \tag{5}$$

The effective hydraulic conductivity $K_{d,\text{eff}}$ (in m s^{-1}) depends on the effective pressure (e.g., Haseloff et al., 2019); ρ_w is the density of water and N_c is a constant (for convenience we use the critical effective pressure for freezing, introduced below). The hydraulic potential Φ is given by

$$\Phi = \rho_w g z_b - N + \rho_i g H. \tag{6}$$

Its gradient drives the water flux. Equation (5) is similar to a model for subglacial conduits eroded into soft beds (Walder and Fowler, 1994).

The basal melt rate m_b satisfies an energy conservation equation,

$$m_b = \frac{1}{\rho_w L_h} \left(q_{\text{geo}} + \tau_b u + k \left. \frac{\partial T}{\partial z} \right|^+ \right), \tag{7}$$

with L_h the latent heat of fusion, q_{geo} the geothermal heat flux, k the thermal conductivity of ice, and $\partial T/\partial z|^+ \approx (T_s - T_m)/H$ the temperature gradient into the ice, which we approximate as linear between surface and melting point temperatures. This assumes that the bed is temperate; this condition is satisfied for all results shown here.

Motivated by observations of thick sediments at the base of the West Antarctic ice sheet (Alley et al., 1986; Anandakrishnan et al., 1998), we assume that water is stored locally in the till, and h_w is proportional to the void ratio e of the till and the thickness of the drained hydraulically active sediment column h_s

$$h_w = \mathrm{e} h_s. \tag{8}$$

The void ratio increases with decreasing effective pressure (Tulaczyk et al., 2000a)

$$\mathrm{e} = \mathrm{e}_r - C_e \log\left(\frac{N + N_0}{N_r}\right) \qquad \text{with } N_0 = N_r \exp\left(\frac{\mathrm{e}_r - \mathrm{e}_0}{C_e}\right). \tag{9}$$

where e_r, e_0, C_e, N_r, and N_0 are constants (see table 1). This relationship is based on the empirical relationship $\mathrm{e} = \mathrm{e}_r - C_e \log(N/N_r)$ between the void ratio of subglacial sediment and effective pressure in the sediment (Tulaczyk et al., 2000a). The constant $N_0 \ll N_r$ has been introduced to satisfy the boundary condition $N = 0$ at the grounding line (13), which now corresponds to a void ratio of e_0. Void ratios in excess of e_0 would correspond to an overpressured system ($N < 0$), but with

https://doi.org/10.5194/egusphere-2025-204
Preprint. Discussion started: 21 February 2025

our choice of parameters this does not happen. We expect that additional model physics would be necessary to capture such a case.

Note that h_s is the thickness of the water-saturated sediment column if all pore space is removed from it ($\mathrm{e} = 0$). As water-filled pores expand the hydraulically active sediment column, its total thickness is $(1+\mathrm{e})h_s = h_s + h_w$ (see figure 1).

2.3 Freezing and melting in the till

Both e and h_s can evolve dynamically and we require a condition in addition to (8) to determine them. This condition comes from the dynamics of freezing and melting in the sediment, which determines the thickness of the hydraulically active sediment layer h_s. We adopt the basal model of Robel et al. (2013, 2014) and Haseloff (2015),

$$\mathrm{e}(N)\frac{\partial h_s}{\partial t} = \begin{cases} m_b & \text{if } \Big(m_b < 0 \text{ and } h_s > 0 \text{ and } (N \geq N_c \text{ or } h_s \leq h_0)\Big) \\ \frac{\mathrm{e}(N)}{\mathrm{e}(N_c)} m_b & \text{if } (m_b > 0 \text{ and } 0 < h_s < h_0) \\ 0 & \text{otherwise.} \end{cases} \tag{10}$$

This condition states that to overcome surface tension and extend the ice surface into the pore space between the grains (corresponding to $h_s < h_0$), the effective pressure must reach a critical value N_c (see e.g., Rempel, 2008, 2009). Therefore, as long as $N < N_c$ and $h_s = h_0$, the pore space expands or consolidates in response to water addition or removal. If freezing occurs while $N < N_c$, then water is removed from the sediment and frozen onto the base of the ice stream (figure 1a). If $N \geq N_c$, freezing results in a frozen fringe, i.e., ice intrudes into the void spaces of the till (figure 1b).

In adopting (10), we make two assumptions that simplify the dynamics of basal freezing. First, once a frozen fringe has formed, any further freezing occurs inside the sediment, even if the effective pressure drops below N_c. This assumption excludes the formation of distinct ice lenses. Second, the void ratio of the frozen sediment is always $\mathrm{e}_c = \mathrm{e}(N_c)$. Theoretically, freezing could occur at smaller void ratios if subglacial drainage has removed water before the onset of freezing so that $N > N_c$. However, melting can readily occur at effective pressures smaller than N_c, accounting for condition $(10)_2$.

Note that our modelling choices prevent the entire basal sediment to freeze ($h_s = 0$). In this case the basal temperature could be below the melting point. This scenario might become important in some areas of Antarctica (Pattyn, 2010; Mantelli et al., 2019). We simultaneously solve for h_w and h_s, with the void ratio e determined from (8) and the effective pressure determined from (9).

2.4 Boundary and initial conditions

We assume an ice divide at $x = 0$ with zero surface slope, velocity and water flux

$$u = \frac{\partial(H+b)}{\partial x} = \frac{\partial \Phi}{\partial x} = 0 \qquad \text{at } x = 0. \tag{11}$$

https://doi.org/10.5194/egusphere-2025-204
Preprint. Discussion started: 21 February 2025

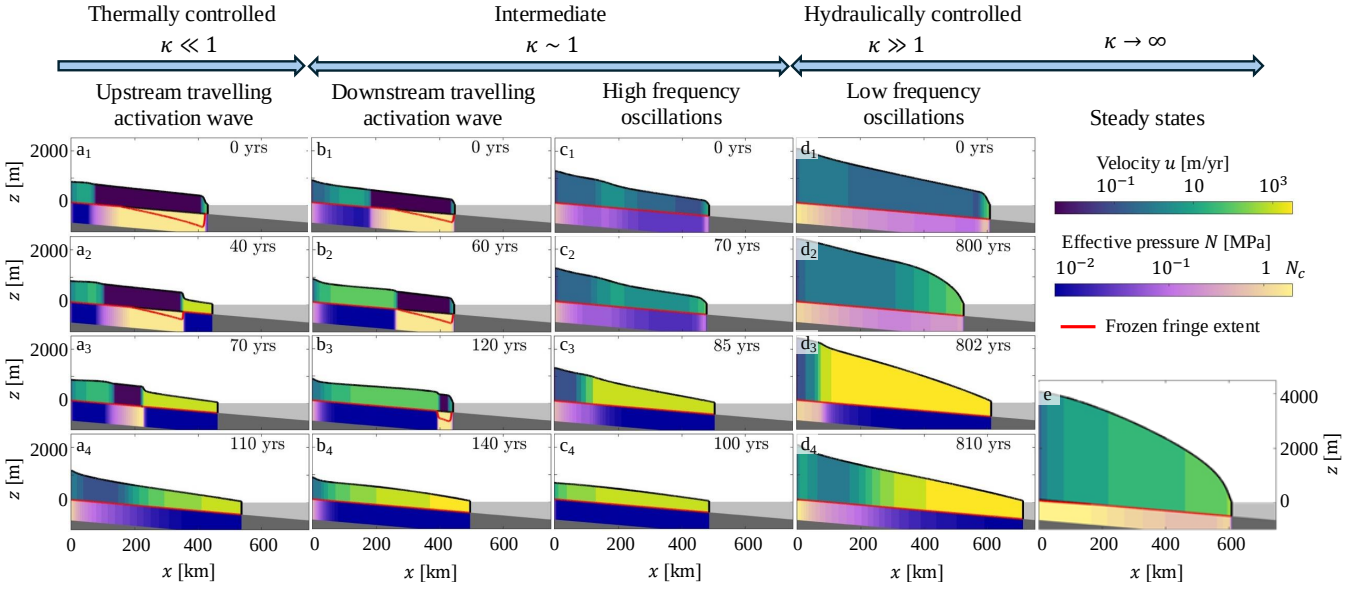

Figure 2. Parameter space of modelled behaviour and sample profiles. Ice is coloured according to speed, and the underlying slab of hydraulically active sediment is coloured according to effective pressure. Note that the thickness of the hydraulically active sediment is vertically exaggerated by 750% and does not account for expansion due to void-ratio changes. The red line indicates the extent of the frozen fringe into the sediment (if located at the ice–bed interface, then there is no frozen fringe). Note the upstream-travelling activation wave of fast flow in column a, the downstream-travelling activation wave in column b, and the quasi-simultaneous speed-up of the entire ice stream in less than two years column d. Animated videos of these solutions are provided as supplementary material.

The position of the grounding line is given through the floatation condition and stress balance condition

$$\left.\begin{aligned} H &= -\frac{\rho_w}{\rho_i} b \\ 2A^{-1/n} H \left|\frac{\partial u}{\partial x}\right|^{1/n-1} \frac{\partial u}{\partial x} &= \frac{1}{2}\rho_i g \left(1 - \frac{\rho_i}{\rho_w}\right) H^2 \end{aligned}\right\} \quad \text{at } x = x_g. \tag{12}$$

We set the effective pressure to zero at the grounding line and assume that the till layer is completely unfrozen where it is in contact with the ocean,

$$N = 0 \quad \text{and} \quad h_s = h_0 \qquad \text{at } x = x_g. \tag{13}$$

For most cases, the model is initialised with a linearly decreasing ice thickness of $H_{\text{initial}} = \max(2000\ \text{m} - 6 \times 10^{-3} x, 100\ \text{m})$, a linearly decreasing effective pressure $N_{\text{initial}} = (20.85 - 10^{-6} \frac{x}{1\text{m}})$ MPa, and $h_s = h_0$. To promote convergence, some runs for $K_d \geq 3 \times 10^{-2}$ m s^{-1} are initialised from solutions previously obtained for other values of K_d.

https://doi.org/10.5194/egusphere-2025-204
Preprint. Discussion started: 21 February 2025

3 Results

We are primarily interested in the interaction of subglacial drainage and ice sheet flow, and therefore consider a suite of models over which hydraulic conductivity decreases from infinity to zero. We expect steady state behaviour at quasi-infinite hydraulic conductivity (e.g., Tsai et al., 2015) and oscillations between slow and fast flow at vanishing hydraulic conductivity (e.g., Robel et al., 2014). Our interest lies in the transition between these limiting cases. In appendix B, we non-dimensionalise the model to show that the non-dimensional group

$$\kappa = \frac{[q_w]/h_0}{[u]} = K_d \times \frac{\mu N_c}{\rho_w g a L_x} \tag{14a}$$

$$\approx K_d \times 10^4 \text{ s m}^{-1} \tag{14b}$$

determines the ice stream behaviour (see figure 2). It describes the ratio between the scale of water velocity $[q_w]/h_0$ and ice velocity $[u]$. For $\kappa \gg 1$, water moves much faster through the subglacial system than the ice sheet evolves, and vice versa. Note that N_c enters (14a) through its appearance in (5), not because of freezing processes.

Ice stream behaviour spans steady streaming ($\kappa \to \infty$), hydraulically controlled oscillations between fast and slow flow ($\kappa \gg 1$), and thermally controlled oscillations ($\kappa \ll 1$). These regimes are distinguished by ice stream morphology, discharge and, where applicable, oscillation frequencies. Notably, hydraulically controlled oscillations are characterised by a quasi-simultaneous speed-up of the entire ice stream (figure 2d), while thermally controlled oscillations exhibit an activation wave, which travels upstream during the speed-up phase (figure 2a). In the regime between these two limiting cases ($\kappa \sim 1$), ice stream activation can occur by downstream propagation of an activation wave (figure 2b). We analyse the processes leading to these different dynamics next, starting with the fully drained limit ($\kappa \to \infty$).

3.1 Steady streaming

In the limit of quasi-infinite conductivity of the hydraulic system, water fluxes are high enough to evacuate melt water efficiently, so that hydraulic gradients ($\partial\Phi/\partial x$) cannot develop, as can be seen from rearranging (5) with (14a),

$$\frac{\partial \Phi}{\partial x} = -\frac{\mu N}{\kappa a L_x h_s} q_w \to 0 \quad \text{for} \quad \kappa \to \infty. \tag{15}$$

Consequently, $\Phi = \rho_w g b - N + \rho_i g H =$ constant. At the grounding line, boundary conditions (12) require $\Phi(x_g) = 0$. This requires the effective pressure to adjust such that $N = \rho_i g H + \rho_w g b$, that is, the subglacial water content is set by the ice and bed geometry alone, and is independent of the basal melt rate (which is positive throughout, see figure 3d$_1$). This leads to high effective pressure and low water content throughout most of the domain (figure 3b$_1$) apart from a small region near the grounding line. Stable steady-state solutions exist, characterised by high ice thickness and surface slopes (figure 3a$_1$). Note that effective pressures in excess of the critical pressure for freezing N_c are possible, as water is removed from the sediment by subglacial drainage, rather than freezing. Here, $\kappa \to \infty$ corresponds to $K_d \approx 10$ m s^{-1}.

As conductivities decrease from infinity, water is less efficiently evacuated, leading to overall higher water content and lower effective pressures, as shown in figure 3b$_{1-3}$. However, basal shear remains high and the average water content increase from

https://doi.org/10.5194/egusphere-2025-204
Preprint. Discussion started: 21 February 2025

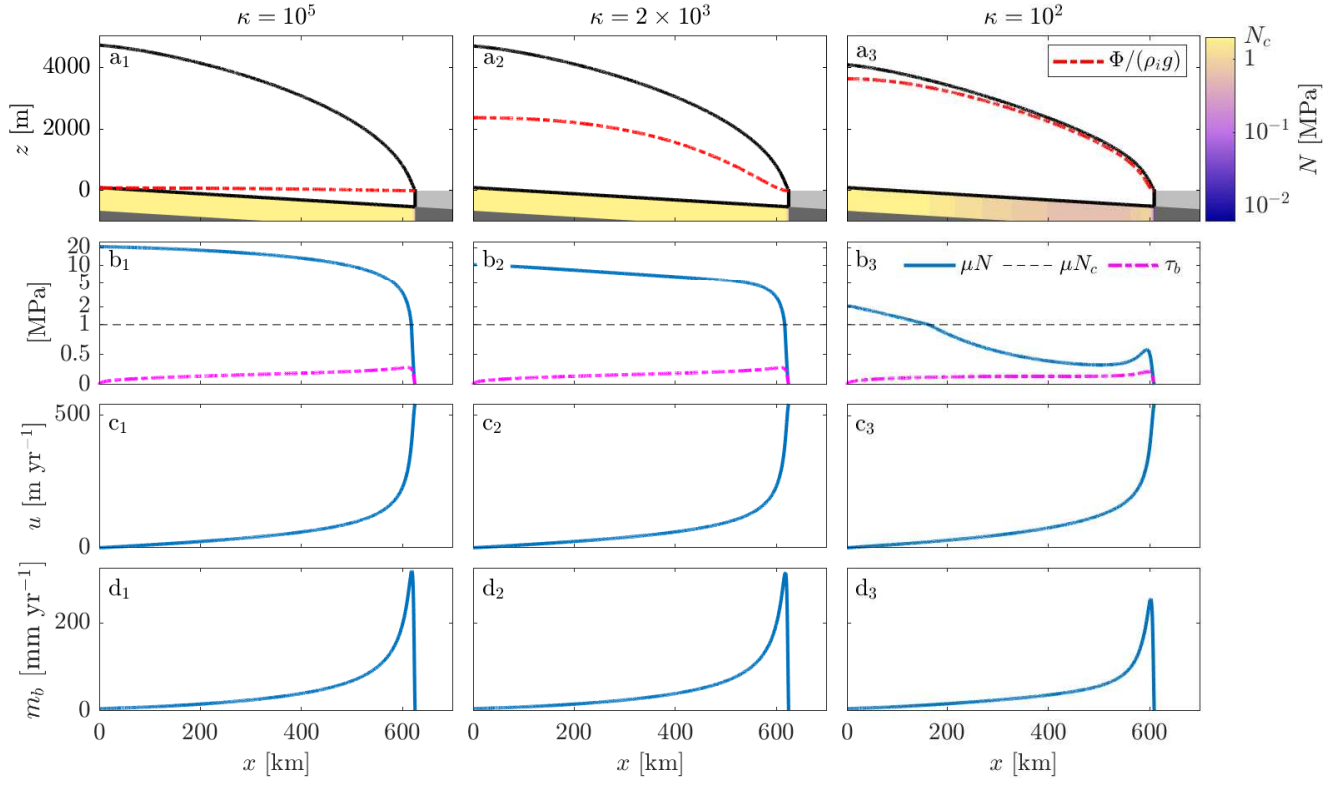

Figure 3. Profiles of hydraulically controlled marine ice sheets with varying values of the hydraulic conductivity of the bed K_d in (5). Top row: ice sheet profile and hydraulic potential Φ. As in figure 2, a vertically exaggerated sediment layer is coloured according to effective pressure. Second row: basal shear stress τ_b and effective pressure contribution μN to it (note that vertical axis is linear below $\mu N_c = 1$ MPa and logarithmic above). Third row: speed. Bottom row: melt rate.

$\bar{h}_w \approx 0.43$ m to $\bar{h}_w \approx 0.53$ m leads to a negligible increase in ice discharge at the grounding line (figure 5c). At $\kappa = 10^2$, a small region of larger effective stress forms just upstream of the grounding line (figure 3b$_3$), corresponding to a lower water content and marginally higher basal resistance.

While this region of elevated effective pressure and basal shear is a subtle feature for the displayed steady state, it becomes critically important for the behaviour at smaller hydraulic conductivities, as steady states cease to exist below a critical value $\kappa \lessapprox 100$. In this range of κ, melt evacuation cannot keep up with melt rates. This leads to an increase in the basal water content and periodic disappearance of the region of elevated basal resistance, and hence to oscillations between fast and slow flow. We analyse the processes leading to these different dynamics next.

https://doi.org/10.5194/egusphere-2025-204
Preprint. Discussion started: 21 February 2025

3.2 Hydraulically controlled oscillations

At moderately high hydraulic conductivity $1 \ll \kappa \lessapprox 100$, basal melt rates are positive in all of the domain, and most of the water is continuously evacuated (figure 4a$_{3,5}$). However, the hydraulic conductivity is not high enough to evacuate all melt water that is produced at the ice–bed interface, and the water content of the bed slowly increases. This shrinks the region of higher basal resistance close to the grounding line (figure 4a$_4$). Eventually the bed is sufficiently weakened for well-lubricated conditions to exist in all of the ice stream, leading to a brief episode of fast flow, enhanced heat dissipation, and sudden grounding line advance. However, a lower effective pressure increases the effective hydraulic conductivity of the bed as $K_{d,\text{eff}} \propto 1/N$ and during this phase more water is discharged than produced. This leads to a strengthening of the bed, eventually restoring the conditions at the beginning of the oscillation cycle. Overall, these oscillations are characterised by short peaks in ice discharge and average water content of the bed (figure 5h$_3$-i$_3$).

Reduction of the hydraulic conductivity decreases the period and amplitude of these oscillations (figure 5). This is due to the mechanical barrier upstream of the grounding line becoming less pronounced (compare the regions of elevated effective pressure in figure 4a$_4$ and b$_4$). At smaller hydraulic conductivity, the subglacial drainage configuration becomes increasingly uncoupled from the hydraulic gradient while the importance of local melting and freezing processes increases (in fact, as the conductivity approaches zero, the subglacial water content is determined by local processes only, as discussed in section 3.4 below). The period of hydraulically controlled oscillations decreases to a minimum of approximately 300 yrs; with further reduction of κ the oscillation period increases again (figure 5).

3.3 Intermediate oscillations

For $\kappa \sim 1$, freezing becomes possible, albeit at first only in a small area close to the grounding line (figure 4b$_3$). However, this has no noticeable effect on the effective pressure and hence basal shear stress as the water flux remains high throughout the domain (figure 4b$_5$). Therefore, for $\kappa = 1$, the ice flow characteristics are similar to those of the hydraulically controlled oscillations, with the entire ice stream speeding up almost simultaneously.

For smaller $\kappa = 10^{-1}$, freezing extends up to the ice divide and leads to strengthening of the bed, which alters the oscillation characteristics. In this case, the onset of fast flow is triggered by the thickening of ice upstream and the ensuing reduction in conductive cooling. This behaviour is shown in panels c$_1$–c$_5$ of figure 4. At the end of the fast-flowing phase, the ice is at its thinnest, basal freezing is prevalent, and a frozen fringe forms in the downstream half of the ice stream. Gradual thickening of ice upstream leads to a transition from basal freezing to melting, decreasing the effective pressure. This leads to faster ice flow in these upstream areas, and thus the formation of a steep surface gradient at the transition between low and high effective stress. The transition between fast and slow flow travels downstream, similar to surge fronts in mountain glaciers (Kamb et al., 1985). While water fluxes generally mirror the inverse of the effective pressure for larger values of κ, here, they are elevated ahead of the downstream travelling surge front (figure 4c$_5$). This indicates that meltwater is transported into the region just downstream of the barrier between low and high effective stress, lowering the effective pressure ahead of the surge front, and thereby allowing its propagation.

https://doi.org/10.5194/egusphere-2025-204
Preprint. Discussion started: 21 February 2025

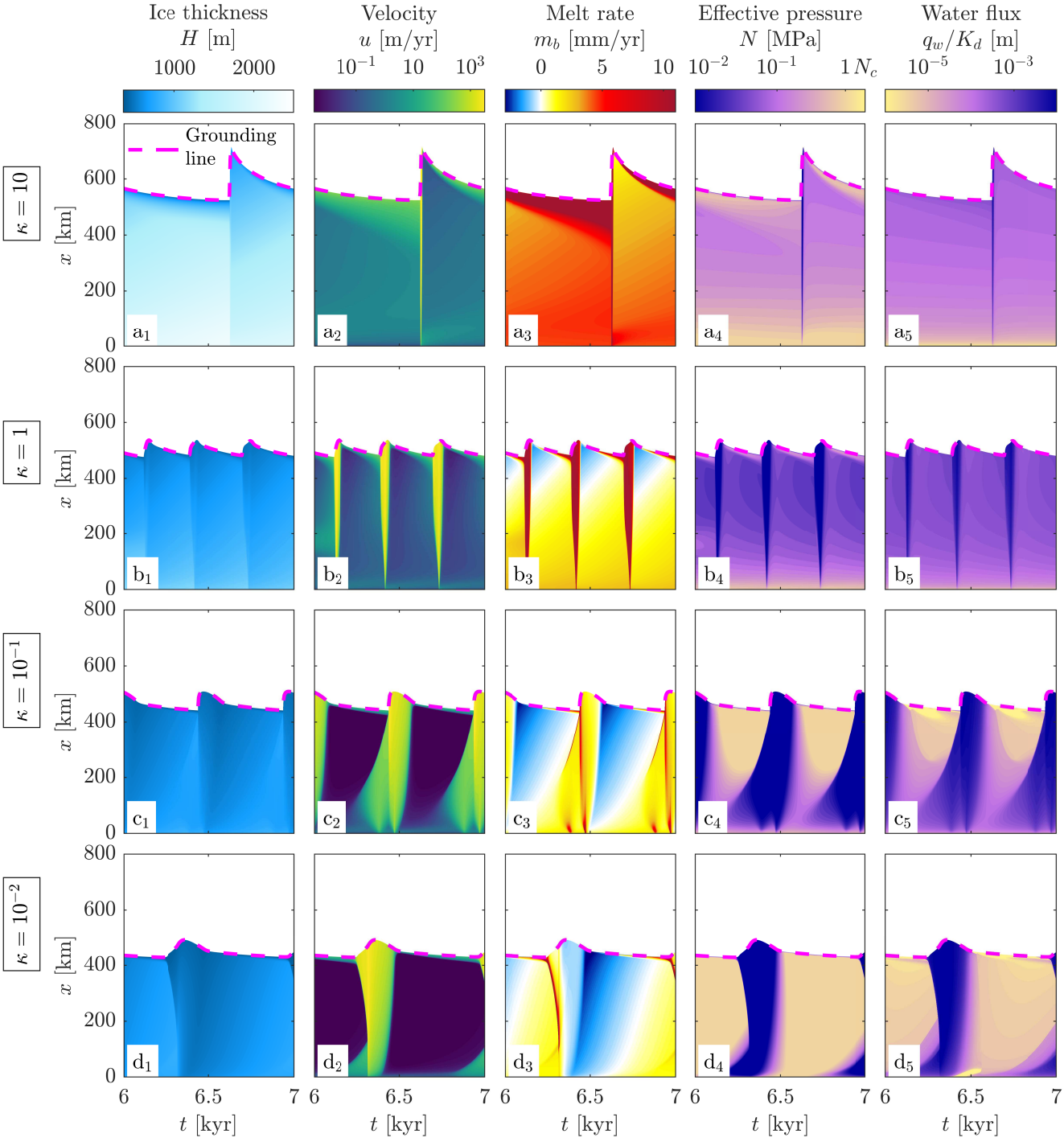

Figure 4. Hovmöller diagrams for four different hydraulic conductivities, decreasing from top to bottom with dashed magenta line marking the grounding-line position. Column 1 shows ice thickness H, column 2 ice velocity u, column 3 melt rate m_b, column 4 effective pressure N, and column 5 the scaled water flux q_w/K_d. Note that the colorbar of the water flux is the inverted colorbar of the effective pressure to facilitate comparison between the two. Animated videos of these solutions are provided as supplementary material.

https://doi.org/10.5194/egusphere-2025-204
Preprint. Discussion started: 21 February 2025

As in the hydraulically controlled oscillations, the region downstream of the surge front acts as a buttress to the overall flow. Once this buttress vanishes, the entire ice stream speeds up, leading to grounding line advance and thinning of the ice stream. The thinner ice stream experiences larger conductive cooling rates, leading to freezing, bed strengthening, and slower flow, closing the oscillation cycle.

3.4 Thermally controlled oscillations

At vanishing hydraulic conductivity ($\kappa \lesssim 10^{-2}$), the conditions at the bed are fully determined by the local energy balance (7), $\partial h_w/\partial t = m_b$. Steady states would require a locally zero melt rate ($m_b = 0$), but this can only occur if conductive cooling exactly balances heat dissipation and geothermal heat flux everywhere. This condition is generally not satisfied. Therefore, the local effective pressure and hence basal resistance to flow change on timescales dependent on the factors controlling the basal melt rate – the heat dissipation ($\tau_b u$ term in (7)) and the conductive cooling ($k\partial T/\partial z|^+$ term in (7)), which in turn is controlled by the ice thickness. This leads to thermally controlled oscillations previously reported in Robel et al. (2014), see figure 4d_1-d_5.

During quasi-stagnant flow phases, the ice is sufficiently thin and slow so that melt rates at the bed are negative and part of the sediment freezes. The effective pressure is at the critical effective pressure for freezing N_c in all of the domain (apart from a small boundary layer close to the grounding line which vanishes for $\kappa \to 0$). Slow flow also means that less mass is evacuated than accumulated and hence the ice sheet thickens over time. This leads to a gradual reduction of the conductive cooling; the energy balance at the bed becomes more positive and the sediment starts to thaw. Once the sediment is fully thawed, further melt produced at the bed is stored locally, leading to a reduction of the effective pressure. As the ice is thicker towards the ice divide, this processes happens first there. However, the flow remains stabilised by the partially frozen sediment in the downstream half of the ice stream.

Eventually, the transition to the fast streaming phase is triggered at the grounding line, where an increase in ice thickness and driving stress leads to speed-up. This increases the heat dissipation, lowers the basal resistance and thus triggers a positive feedback between fast flow, heat dissipation, and basal lubrication. Force balance dictates that loss of basal resistance to flow affects the flow in a small boundary layer immediately upstream through longitudinal stresses ($\eta\partial u/\partial x$, see e.g., Robel et al., 2014). At high effective stress this boundary layer dissipates significant heat, quickly lowering its own effective pressure, which then speeds up the flow immediately upstream. This creates an activation wave that travels upstream, which is clearly visible in the melt rate (figure 4d_3); its properties are discussed in detail in Robel et al. (2014). In its wake the ice stream bed is well-lubricated, leading to discharge of ice in excess of accumulation, thinning of the ice, and consequently increasing conductive cooling at the bed. This eventually leads to strengthening of the bed, slow down of flow, and transition to the stagnant phase. The frequency of these oscillations is primarily determined by how fast the ice stream can replenish its mass (i.e., the accumulation rate) and the terms in the melt rate (7) (i.e., k, T_s and q_{geo}, MacAyeal, 1993; Robel et al., 2013).

https://doi.org/10.5194/egusphere-2025-204
Preprint. Discussion started: 21 February 2025

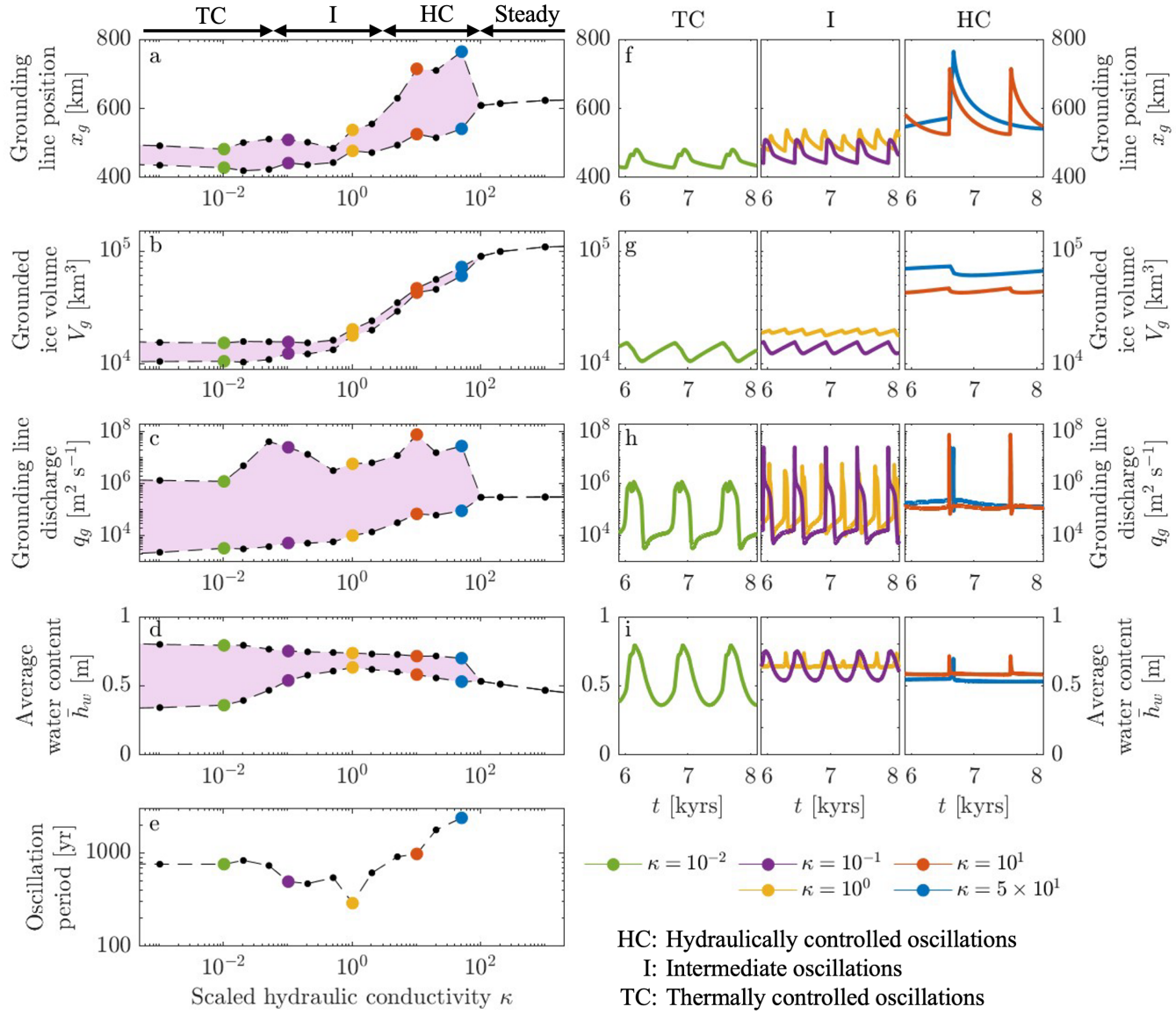

Figure 5. Bifurcation diagrams for finite κ (panels a-e) and selected time series after an initial spin up of 6000 years (panels f-i). Shaded area in plots a-d corresponds to the range covered during an oscillation period; points are minimum and maximum values of the oscillation. Note that hydraulically controlled oscillations are characterised by a sharp peak in discharge and water content (e.g., red curves in plot h and i), while thermally controlled oscillations are changing more gradually (e.g., green curve in plot h and i).

https://doi.org/10.5194/egusphere-2025-204
Preprint. Discussion started: 21 February 2025

4 Discussion

In this study, we investigate the role of an evolving subglacial drainage system on marine ice stream dynamics using the simplest model of the relevant physics. A positive feedback between fast flow and basal lubrication is incorporated through both increasing local storage of water with decreasing effective pressure and increasing drainage efficiency with decreasing effective pressure. Subglacial conditions affect marine ice sheet dynamics through the basal shear stress, which depends on the effective pressure.

We find that the efficiency of subglacial drainage controls the mode of grounding line dynamics. Lower hydraulic conductivities result in lower basal resistance and faster flow, i.e., generally higher slip rates, thinner ice, and less grounded ice volume (figure 5b). With lower hydraulic conductivities, the melt rate at the bed gradually drops, from positive at all points in space and time (due to thicker ice mitigating conductive cooling) to zero on average at the impermeable limit, see figure $4a_4$-d_4. This behaviour is accompanied by a transition from a quasi-simultaneous speed-up of the entire ice stream to a gradual speed-up and slowdown (figure 5h). This speed-up can be due to downstream and upstream-travelling activation waves.

4.1 Ice stream oscillations and glacier surges

The similarities of the marine ice streams modelled here and the observed behaviour of surging glaciers corroborate the hypothesis that the same dynamics govern both of these systems, albeit at different spatial and temporal scales (e.g., Clarke et al., 1984). In the regime intermediate between hydraulical and thermal control, the oscillations share similarities with the observed classical surges of Varigated Glacier, Trapridge Glacier and others: a downstream-travelling surge front, acceleration by up to three orders of magnitude, and a basal gradient between upstream temperate conditions and downstream near-frozen bed conditions (Clarke et al., 1984; Kamb et al., 1985). Recent observations have also shown that some surges are instead characterised by upwards travelling activation waves (Murray et al., 2003; Sevestre et al., 2018), leading to the hypothesis that there are at least two distinct surge mechanisms (Murray et al., 2003). Our results suggest that these different surge dynamics could be due to small variations in effective basal conductivity of the bed.

Previous conceptual, non-spatial ("lumped") models for surging glaciers (Fowler et al., 2001; Benn et al., 2019, 2022; Terleth et al., 2024) include the same ingredients as our model. These models show that the existence of oscillations also depends on climatic (accumulation, surface temperature) and geometric factors (bed slope). While our focus is on the dynamic behaviour resulting from variable hydraulic conductivity, it is reasonable to assume that variation of climatic and geometric factors will have an equally important effect on marine ice-stream dynamics in our model. Conversely, we supplement existing, zero-dimensional models for glacier surges with a spatially extended model, enabling identification and analysis of previously inaccessible complexities.

https://doi.org/10.5194/egusphere-2025-204
Preprint. Discussion started: 21 February 2025

4.2 Marine ice sheet dynamics

Marine ice sheet dynamics are typically framed to be either stable or unstable, with instability equated to marine ice sheet collapse. Our results indicte that such classifications do not hold if basal boundary conditions can dynamically evolve. Instead, marine ice streams might undergo periodic cycles of retreat and re-advance.

Most models simulating future ice loss under warming scenarios do not account for evolving basal boundary conditions. Our results show that basal conditions can change within a few hundred years. Faster oscillations are likely possible for different parameter choices. However, incorporation of subglacial drainage into predictive ice-sheet models is still hampered by uncertainty how subglacial drainage should be upscaled to large spatial and temporal scales, as well as the computational cost of incorporating these dynamics.

4.3 Subglacial hydrology of ice streams

Given the control that effective conductivity of the bed exerts on ice stream dynamics, determining appropriate parameterizations of the effective hydraulic conductivity is crucial. Estimates of hydraulic conductivity of till vary between 10^{-9} to 5×10^{-5} m s^{-1} for different locations (Fountain and Walder, 1998). However, these values are not straightforwardly transferable to the values of K_d used here. These values do not take the formation of subglacial conduits into account. Such conduits likely increase the effective hydraulic conductivity and introduce a dependence on the effective pressure. For example, slug tests have yielded enhanced hydraulic conductivities of unconsolidated sediments close to a subglacial channel (from 10^{-3} to 10^{-2} m s^{-1}, Kulessa et al., 2005).

More generally, modelling West Antarctic basal environments requires models for water flow on soft (permeable and deformable) beds. Most subglacial drainage models are developed for hard (impermeable and undeformable) beds, but the existence of subglacial till beneath parts of West Antarctica is well established (Blankenship et al., 1986, 1987; Alley et al., 1986; Alley et al., 1987; Peters et al., 2006). Based on these observations, Walder and Fowler (1994) and Ng (2000) propose the existence of subglacial canals partially eroded into the bed and ice. In settings typical for ice streams, the dynamics of these conduits mimic those typical for distributed subglacial systems where the effective pressure decreases with increasing water discharge. Assuming the same qualitative behaviour as Walder and Fowler (1994), we have used $K_{d,\text{eff}} \propto 1/N$. However, a more complicated relationship is not only possible but likely for realistic ice streams, where a range of subglacial drainage systems might exist at the same value of N (Flowers, 2015). In particular, it is plausible that the net discharge increases with effective pressure, rather than decreases. Such a scenario could occur in a highly channelised subglacial drainage system (Röthlisberger, 1972). In Greenland, where abundant meltwater can drain to the bed, increasing channelisation leads to a strengthening of the bed at the end of the melt season (Schoof, 2010; Bartholomew et al., 2012). We would also expect the conductivity to vary locally, so that we interpret $K_{d,\text{eff}}$ as an effective hydraulic conductivity, averaged over spatial scales resolvable in ice sheet models.

We have assumed that the basal shear stress adjusts instantaneously to changes in subglacial water content, as we are interested in the annual to centennial evolution of marine ice sheets. However, at the grounding line, marine ice sheets are subject

https://doi.org/10.5194/egusphere-2025-204
Preprint. Discussion started: 21 February 2025

to tidal forcing on much shorter timescales. At such short timescales, transient dilatant strengthening of subglacial till can lead to time-dependent sliding laws and affect grounding line motion (Warburton et al., 2020, 2023). It has been hypothesised that time-dependent sliding laws might also modulate surging of glaciers (Minchew and Meyer, 2020); this behaviour might be important for the quasi-simultaneous speed-up we observed in the hydraulically controlled limit at moderately high hydraulic conductivities.

4.4 Model limitations

In the formulation of our model, we have made simplifying assumptions that limit its applicability. Most notably, we use a width-integrated model with a parameterized lateral drag term. Assuming that the width of the ice stream is constant allows us to ignore the complex dynamics required to capture its evolution. However, observations indicate that ice-stream widths can change over time (e.g., Harrison et al., 1998; Echelmeyer and Harrison, 1999). Modelling also shows that substantial melt is produced in ice-stream margins, which could affect ice stream hydrology and dynamics (Raymond, 2000; Suckale et al., 2014; Haseloff et al., 2019). Future modelling efforts should build on our work to account for the hydraulic and thermal processes affecting ice stream width.

Another limitation of the width-averaged approach is that it precludes the formation of ice ridges, whose surface slopes affect the ice stream stability by altering the hydraulic gradient (Kyrke-Smith et al., 2014). The advantage is that we are left with a minimal model of a marine ice stream in which dissipation, drainage, and freezing processes compete to shape the ice stream thickness and velocity field, and we can study the effect of different physical processes in the model.

We also ignore the role of ice shelves here. Buttressing ice shelves can alter marine ice stream dynamics (Gudmundsson et al., 2012; Gudmundsson, 2013; Haseloff and Sergienko, 2018, 2022). Such effects should be addressed in future studies.

Another model limitation is that we do not allow for full freezing of the bed; in all simulations reported here the bed remains temperate. Observations suggest temperate ice stream beds (e.g., Engelhardt and Kamb, 1997) but the bed might be frozen under the adjacent ice ridges (e.g., Bentley et al., 1998). Frozen–temperate transitions might also play a role in ice stream onset (Mantelli et al., 2019), although in our model upstream regions usually have higher water content, as the thicker ice there reduces conductive cooling of the bed. The formation of temperate to frozen boundaries is not possible in our model, and additional model physics would be required to capture these (Haseloff et al., 2015, 2018; Mantelli and Schoof, 2019; Schoof and Mantelli, 2021).

5 Conclusions

In this paper we showed that subglacial hydrology affects the stability, extent, and grounded ice volume of marine ice streams. Different dynamical regimes, including steady streaming, hydraulically controlled, quasi-simultaneous advances, periodic surges with advancing or retreating activation fronts, and thermally controlled oscillations are possible for different hydraulic conductivities of the bed. Our results illustrate that marine ice streams can undergo internal variability at periods up to a few

https://doi.org/10.5194/egusphere-2025-204
Preprint. Discussion started: 21 February 2025

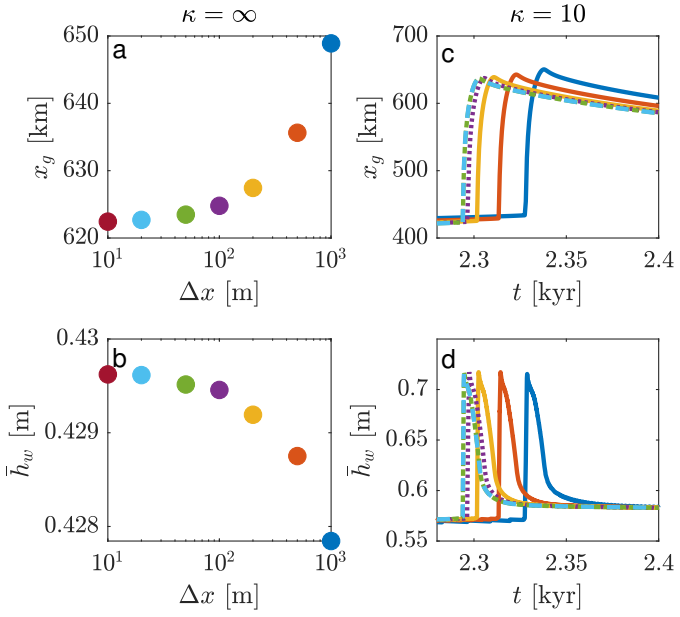

Figure A1. Numerical convergence study. Panels a-b show grounding line position x_g and average water content $\bar{h}_w$ under grid refinement for steady-state solutions ($\kappa = \infty$), panels c-d show the same for oscillating solutions ($\kappa = 10$).

centuries. This variability may need to be taken into account for accurate prediction of future sea level contributions on these timescales.

Code availability. The PETSc code used in this study will be deposited on Zenodo upon revision of this paper.

Video supplement. https://av.tib.eu/series/1864 (Haseloff et al., 2025)

Appendix A: Model implementation and verification

The model is implemented in PETSc (Balay et al., 2023) using finite differences on a fixed staggered grid with an implicit time-step. The implemented scheme is of $O(\Delta x)$, and comparison of steady-state results and timeseries under grid refinement are shown in figure A1. While the qualitative behaviour is consistent for values of $\Delta x \lesssim 1000$ m, convergence requires resolution at 10s of meters. Solutions shown here were calculated at resolutions of $\Delta x = 100$ m or finer.

https://doi.org/10.5194/egusphere-2025-204
Preprint. Discussion started: 21 February 2025

Appendix B: Non-dimensional model

Here, we non-dimensionalize equations (1)–(4) to highlight scaling behaviour in each balance region. There are two limiting cases. For hydraulically controlled ice streams, ice is relatively thick, velocities are slow, and basal resistance is high, with both the Weertman-like terms and the Coulomb-like terms in equation (3) contributing to the basal shear stress. Subglacial water flow is efficient and the sediment does not experience freezing. We consider this limit first in section B1. For thermally controlled ice streams, ice is thin and basal resistance is primarily of the Coulomb-plastic type. The basal energy balance oscillates between melting and freezing; this limit is considered below in section B2.

B1 Hydraulically controlled ice streams

In this limit, we choose the following scales with characteristic values as indicated,

$$[x] = L_x = 1000 \text{ km}, \tag{B1a}$$

$$[u] = \left(\frac{\rho_i g a^2 [x]}{C}\right)^{n/(2n+1)} \approx 60 \text{ m yr}^{-1}, \tag{B1b}$$

$$[H] = \frac{a[x]}{[u]} \approx 4700 \text{ m}, \tag{B1c}$$

$$[t] = \frac{[H]}{a} \approx 15 \times 10^3 \text{ yr}, \tag{B1d}$$

$$[N] = \frac{1}{\mu} C [u]^{1/n} \approx 400 \text{ kPa}. \tag{B1e}$$

We set $x = [x]x^*$, $H = [H]H^*$, $u = [u]u^*$, $t = [t]t^*$, $N = [N]N^*$, $h_s = h_0 h_s^*$, and $\Phi = \rho_i g [H] \Phi^*$. Dropping asterisks immediately, we obtain the non-dimensional equations for momentum balance (2), mass balance (1), and water balance (4),

$$2\alpha_1 \frac{\partial}{\partial x}\left(H \left|\frac{\partial u}{\partial x}\right|^{1/n-1} \frac{\partial u}{\partial x}\right) - \alpha_2 H u^{1/n} - \frac{N u^{1/n}}{u^{1/n} + N} \frac{u}{|u|} = H \frac{\partial H}{\partial x} \tag{B2a}$$

$$\frac{\partial H}{\partial t} + \frac{\partial (uH)}{\partial x} = 1 \tag{B2b}$$

$$\frac{\partial (e h_s)}{\partial t} + \kappa \frac{\partial}{\partial x}\left(\frac{1}{N}\frac{\partial \Phi}{\partial x}\right) = \left(\alpha_3 + \alpha_4 \frac{N u^{1/n+1}}{u^{1/n} + N} - \alpha_5 \frac{1}{H}\right) \tag{B2c}$$

https://doi.org/10.5194/egusphere-2025-204
Preprint. Discussion started: 21 February 2025

with the non-dimensional groups

$$\alpha_1 = \frac{[H]}{A^{1/n} C L_x^{1/n+1}} \approx 3 \times 10^{-4}, \tag{B3a}$$

$$\alpha_2 = \frac{C_w [H]}{A^{1/n} C W^{1/n+1}} \approx 4 \times 10^{-2}, \tag{B3b}$$

$$\kappa = K_d \frac{\mu N_c}{\rho_w g L_x a} \approx K_d \times 10^4 \text{ s m}^{-1}, \tag{B3c}$$

$$\alpha_3 = \frac{q_{\text{geo}} [H]}{\rho_w L_h h_0 a} \approx 100, \tag{B3d}$$

$$\alpha_4 = \frac{C [u]^{1/n} [x]}{\rho_w L_h h_0} \approx 600, \tag{B3e}$$

$$\alpha_5 = \frac{k \Delta T}{\rho_w L_h h_0 a} \approx 13. \tag{B3f}$$

With $\alpha_1 \ll \alpha_2 \ll 1$, the leading order momentum balance is between basal resistance and driving stress,

$$-\frac{N u^{1/n}}{u^{1/n} + N} \frac{u}{|u|} \sim H \frac{\partial H}{\partial x}. \tag{B4}$$

In the basal water balance, the non-dimensional group of interest is κ, which controls the importance of subglacial hydrology. It can be understood at the ratio of subglacial water velocity to ice velocity, as

$$\kappa = \frac{[q_w]/h_0}{[u]} \quad \text{with} \quad [q_w] = K_d \frac{N_c h_0 [\Phi]}{\rho_w g [N] [x]}. \tag{B5}$$

If $K_d \sim (\rho_w g L_x a)/(\mu N_c)$, then $\kappa \sim 1$. We also note that $\alpha_5 \ll \alpha_4$, i.e., freezing is negligible.

For $\kappa \to \infty$, we expect steady-states with constant hydraulic potential as detailed in (15). Practically, this limit is attained for $K_d \sim 10$ m s^{-1} (corresponding to $\kappa \approx 10^5$). As long as $\kappa \gg 1$, we expect subglacial hydrology to be efficient; we call this limit hydraulically controlled. In this case, the leading order water balance is

$$\kappa \frac{\partial}{\partial x} \left(\frac{1}{N} \frac{\partial \Phi}{\partial x} \right) \sim \alpha_4 \frac{N u^{1/n+1}}{u^{1/n} + N}. \tag{B6}$$

For $\kappa \ll 1$ we expect subglacial hydrology to become increasingly ineffective and the interplay between local melt production and freezing to dominate the basal energy balance. This requires thinner ice streams; we rescale below to capture this asymptotic limit.

The limit $\kappa \sim 1$ describes the intermediate regime. In this limit, the relative magnitudes of subglacial water flux, geothermal heat flux, basal energy dissipation, and conductive cooling determine the energy balance.

https://doi.org/10.5194/egusphere-2025-204
Preprint. Discussion started: 21 February 2025

B2 Thermally controlled ice streams

In this limit, we choose the following scales

$$[x] = L_x = 1000 \text{ km}, \tag{B7a}$$

$$[H] = \frac{k\Delta T}{q_{\text{geo}}} \approx 600 \text{ m}, \tag{B7b}$$

$$[u] = \frac{a[x]}{[H]} \approx 500 \text{ m yr}^{-1}, \tag{B7c}$$

$$[t] = \frac{[H]}{a} \approx 2000 \text{ yr}, \tag{B7d}$$

$$[N] = \frac{1}{\mu}\rho_i g \frac{[H]^2}{[x]} \approx 7 \text{ kPa}. \tag{B7e}$$

We set $x = [x]x^\dagger$, $H = [H]H^\dagger$, $u = [u]u^\dagger$, $t = [t]t^\dagger$, $N = [N]N^\dagger$, $h_s = h_0 h_s^*$, and $\Phi = \rho_i g[H]\Phi^\dagger$. Dropping daggers immediately, we obtain the non-dimensional equations for mass balance (1), momentum balance (2), and water balance (4),

$$2\gamma_1 \frac{\partial}{\partial x}\left(H\left|\frac{\partial u}{\partial x}\right|^{1/n-1}\frac{\partial u}{\partial x}\right) - \gamma_2 H u^{1/n} - \frac{\gamma_3 N u^{1/n}}{\gamma_3 u^{1/n} + N}\frac{u}{|u|} = H\frac{\partial H}{\partial x} \tag{B8a}$$

$$\frac{\partial H}{\partial t} + \frac{\partial (uH)}{\partial x} = 1 \tag{B8b}$$

$$\frac{\partial (eh_s)}{\partial t} + \kappa \frac{\partial}{\partial x}\left(\frac{1}{N}\frac{\partial \Phi}{\partial x}\right) = \gamma_4\left(1 - \frac{1}{H}\right) + \gamma_5 \frac{\gamma_3 N u^{1/n+1}}{\gamma_3 u^{1/n} + N} \tag{B8c}$$

with non-dimensional groups

$$\gamma_1 = \frac{a^{1/n}}{\rho_i g A^{1/n}[H]^{1/n+1}} \approx 4 \times 10^{-3}, \tag{B9a}$$

$$\gamma_2 = C_w\left(\frac{[x]}{W}\right)^{1/n+1}\gamma_1 \approx 0.7, \tag{B9b}$$

$$\gamma_3 = \frac{C a^{1/n}[x]^{1/n+1}}{\mu \rho_i g [H]^{2+1/n}} \approx 120, \tag{B9c}$$

$$\gamma_4 = \frac{1}{\rho_w L_h}\frac{k\Delta T}{a h_0} \approx 13, \tag{B9d}$$

$$\gamma_5 = \frac{\rho_i g}{\rho_w L_h h_0}\left(\frac{k\Delta T}{q_{\text{geo}}}\right)^2 \approx 10. \tag{B9e}$$

As before, the dimensional group determining the role of subglacial hydrology is κ. Subglacial water flux is negligible for $\kappa \ll 1$ which describes thermally controlled oscillations. In this limit the leading order water balance (neglecting terms of $O(1/\gamma_3)$) is

$$\frac{\partial (eh_s)}{\partial t} \sim \gamma_4\left(1 - \frac{1}{H}\right) + \gamma_5 N u. \tag{B10}$$

This limit is attained for $K_d \lessapprox 10^{-6}$ m s^{-1}.

https://doi.org/10.5194/egusphere-2025-204
Preprint. Discussion started: 21 February 2025

Author contributions. MH designed the study, formulated the model, performed the research, and wrote the manuscript. IJH advised on the model formulation and interpretation. RFK advised on the numerical solution of the model. All authors secured funding for part of the project and contributed to the editing of the manuscript.

Competing interests. The authors declare no competing interests.

Acknowledgements. This study was supported by award NSF2218463 from the National Science Foundation and NERC Grant NE/R000026/1.

https://doi.org/10.5194/egusphere-2025-204
Preprint. Discussion started: 21 February 2025

References

Alley, R. B., Blankenship, D. D., Bentley, C. R., and Rooney, S. T.: Deformation of till beneath ice stream B, West Antarctica, Nature, 322, 57–59, https://doi.org/10.1038/322057a0, 1986.

Alley, R. B., Blankenship, D., Bentley, C., and Rooney, S.: Till beneath ice stream B, 3, Till deformation: Evidence and implications, Journal of Geophysical Research, 92, 8921–8930, doi:10.1029/JB092iB09p08 921, 1987.

Anandakrishnan, S. and Alley, R. B.: Stagnation of ice stream C, West Antarctica by water piracy, Geophysical Research Letters, 24, 265–268, doi:10.1029/96GL04 016, 1997.

Anandakrishnan, S., Blankenship, D. D., Alley, R. B., and Stoffa, P. L.: Influence of subglacial geology on the position of a West Antarctic ice stream from seismic observations, Nature, 394, 62–65, doi:10.1038/27 889, https://doi.org/10.1038/27889, 1998.

Balay, S., Abhyankar, S., Adams, M. F., Benson, S., Brown, J., Brune, P., Buschelman, K., Constantinescu, E. M., Dalcin, L., Dener, A., Eijkhout, V., Faibussowitsch, J., Gropp, W. D., Hapla, V., Isaac, T., Jolivet, P., Karpeev, D., Kaushik, D., Knepley, M. G., Kong, F., Kruger, S., May, D. A., McInnes, L. C., Mills, R. T., Mitchell, L., Munson, T., Roman, J. E., Rupp, K., Sanan, P., Sarich, J., Smith, B. F., Zampini, S., Zhang, H., Zhang, H., and Zhang, J.: PETSc Web page, https://petsc.org/, https://petsc.org/, 2023.

Bartholomew, I., Nienow, P., Sole, A., Mair, D., Cowton, T., and King, M. A.: Short-term variability in Greenland Ice Sheet motion forced by time-varying meltwater drainage: Implications for the relationship between subglacial drainage system behavior and ice velocity, Journal of Geophysical Research: Earth Surface, 117, https://doi.org/10.1029/2011JF002220, 2012.

Benn, D. I., Fowler, A. C., Hewitt, I., and Sevestre, H.: A general theory of glacier surges, Journal of Glaciology, 65, 701–716, 2019.

Benn, D. I., Hewitt, I. J., and Luckman, A. J.: Enthalpy balance theory unifies diverse glacier surge behaviour, Annals of Glaciology, 63, 88–94, 2022.

Bentley, C. R., Lord, N., and Liu, C.: Radar reflections reveal a wet bed beneath stagnant Ice Stream C and a frozen bed beneath ridge BC, West Antarctica, Journal of Glaciology, 44, 149–156, 1998.

Bindschadler, R. and Vornberger, P.: Changes in the West Antarctic Ice Sheet Since 1963 from Declassified Satellite Photography, Science, 279, 689–692, doi:10.1126/science.279.5351.689, https://doi.org/10.1126/science.279.5351.689, 1998.

Blankenship, D. D., Bentley, C. R., Rooney, S. T., and Alley, R. B.: Seismic measurements reveal a saturated porous layer beneath an active Antarctic ice stream, Nature, 322, 54–57, https://doi.org/10.1038/322054a0, 1986.

Blankenship, D. D., Bentley, C. R., Rooney, S. T., and Alley, R. B.: Till beneath ice stream B. I - Properties derived from seismic travel times. II - Structure and continuity. III - Till deformation - Evidence and implications. IV - A coupled ice-till flow model, Journal of Geophysical Research, 92, 8903–8940, https://doi.org/10.1029/JB092iB09p08903, 1987.

Bougamont, M., Tulaczyk, S., and Joughin, I.: Numerical investigations of the slow-down of Whillans Ice Stream, West Antarctica: is it shutting down like Ice Stream C?, Annals of Glaciology, 37, 239–246, https://doi.org/10.3189/172756403781815555, 2003.

Bougamont, M., Price, S., Christoffersen, P., and Payne, A.: Dynamic patterns of ice stream flow in a 3-D higher-order ice sheet model with plastic bed and simplified hydrology, Journal of Geophysical Research: Earth Surface, 116, 2011.

Brinkerhoff, D. J. and Johnson, J. V.: Dynamics of thermally induced ice streams simulated with a higher-order flow model, Journal of Geophysical Research, 120, 1743–1770, https://doi.org/10.1002/2015JF003499, 2015JF003499, 2015.

Brondex, J., Gagliardini, O., Gillet-Chaulet, F., and Durand, G.: Sensitivity of grounding line dynamics to the choice of the friction law, Journal of Glaciology, 63, 854–866, https://doi.org/10.1017/jog.2017.51, 2017.

https://doi.org/10.5194/egusphere-2025-204
Preprint. Discussion started: 21 February 2025

Catania, G., Hulbe, C., Conway, H., Scambos, T. A., and Raymond, C. F.: Variability in the mass flux of the Ross ice streams, West Antarctica, over the last millennium, Journal of Glaciology, 58, 741–752, https://doi.org/10.3189/2012JoG11J219, 2012.

Christoffersen, P. and Tulaczyk, S.: Response of subglacial sediments to basal freeze-on 1. Theory and comparison to observations from beneath the West Antarctic Ice Sheet, Journal of Geophysical Research, 108, 2222, https://doi.org/10.1029/2002JB001935, 2003.

Clarke, G. K., Collins, S. G., and Thompson, D. E.: Flow, thermal structure, and subglacial conditions of a surge-type glacier, Canadian Journal of Earth Sciences, 21, 232–240, https://doi.org/10.1139/e84-024, 1984.

Clarke, G. K. C.: Subglacial Processes, Annual Review of Earth and Planetary Sciences, 33, 247–276, 2005.

Clarke, G. K. C., Nitsan, U., and Paterson, W. S. B.: Strain heating and creep instability in glaciers and ice sheets, Reviews of Geophysics, 15, 235–247, https://doi.org/10.1029/RG015i002p00235, 1977.

Dupont, T. K. and Alley, R. B.: Assessment of the importance of ice-shelf buttressing to ice-sheet flow, Geophysical Research Letters, 32, 4503–+, https://doi.org/10.1029/2004GL022024, 2005.

Echelmeyer, K. A. and Harrison, W. D.: Ongoing margin migration of Ice Stream B, Antarctica, Journal of Glaciology, 45, 361–369, https://doi.org/10.3189/S0022143000001866, 1999.

Elsworth, C. W. and Suckale, J.: Rapid ice flow rearrangement induced by subglacial drainage in West Antarctica, Geophysical Research Letters, 43, 11–697, https://doi.org/10.1002/2016GL070430, 2016.

Engelhardt, H. and Kamb, B.: Basal hydraulic system of a West Antarctic ice stream: constraints from borehole observations, Journal of Glaciology, 43, 207–230, 1997.

Feldmann, J. and Levermann, A.: From cyclic ice streaming to Heinrich-like events: the grow-and-surge instability in the Parallel Ice Sheet Model, The Cryosphere, 11, 1913–1932, https://doi.org/10.5194/tc-11-1913-2017, 2017.

Flowers, G. E.: Modelling water flow under glaciers and ice sheets, Proceedings of the Royal Society of London A: Mathematical, Physical and Engineering Sciences, 471, https://doi.org/10.1098/rspa.2014.0907, 2015.

Fountain, A. G. and Walder, J. S.: Water flow through temperate glaciers, Reviews of Geophysics, 36, 299–328, https://doi.org/10.1029/97RG03579, 1998.

Fowler, A., Murray, T., and Ng, F.: Thermally controlled glacier surging, Journal of Glaciology, 47, 527–538, https://doi.org/10.3189/172756501781831792, 2001.

Fowler, A. C. and Johnson, C.: Ice-sheet surging and ice-stream formation, Annals of Glaciology, 23, 68–73, 1996.

Fowler, A. C. and Schiavi, E.: A theory of ice-sheet surges, Journal of Glaciology, 44, 104–118, 1998.

Fricker, H. A., Scambos, T., Bindschadler, R., and Padman, L.: An Active Subglacial Water System in West Antarctica Mapped from Space, Science, 315, 1544–1548, https://doi.org/10.1126/science.1136897, 2007.

Gudmundsson, G. H.: Ice-shelf buttressing and the stability of marine ice sheets, The Cryosphere, 7, 647–655, https://doi.org/10.5194/tc-7-647-2013, 2013.

Gudmundsson, G. H., Krug, J., Durand, G., Favier, L., and Gagliardini, O.: The stability of grounding lines on retrograde slopes, The Cryosphere, 6, 1497–1505, https://doi.org/10.5194/tc-6-1497-2012, 2012.

Harrison, W. D., Echelmeyer, K. A., and Larsen, C. F.: Measurement of temperature in a margin of Ice Stream B, Antarctica: implications for margin migration and lateral drag, Journal of Glaciology, 44, 615–624, 1998.

Haseloff, M.: Modelling the migration of ice stream margins, Ph.D. thesis, The University of British Columbia, doi: 10.14288/1.0166470, https://doi.org/10.14288/1.0166470, 2015.

https://doi.org/10.5194/egusphere-2025-204
Preprint. Discussion started: 21 February 2025

Haseloff, M. and Sergienko, O. V.: The effect of buttressing on grounding line dynamics, Journal of Glaciology, 64, 417–431, https://doi.org/10.1017/jog.2018.30, 2018.

Haseloff, M. and Sergienko, O. V.: Effects of calving and submarine melting on steady states and stability of buttressed marine ice sheets, Journal of Glaciology, 68, 1149–1166, https://doi.org/10.1017/jog.2022.29, 2022.

Haseloff, M., Schoof, C., and Gagliardini, O.: A boundary layer model for ice stream margins, Journal of Fluid Mechanics, 781, 353–387, https://doi.org/10.1017/jfm.2015.503, 2015.

Haseloff, M., Hewitt, I. J., and Katz, R. F.: Englacial pore-water localises shear in temperate ice-stream margins, Journal of Geophysical Research: Earth Surface, https://doi.org/10.1029/2019JF005399, 2019.

Haseloff, M., Hewitt, I. J., and Katz, R. F.: Supplemental videos for the paper "Subglacial hydrology regulates oscillations in marine ice streams", Copernicus Publications, https://av.tib.eu/series/1864, 2025.

Haseloff, M., Schoof, C., and Gagliardini, O.: The role of subtemperate slip in thermally driven ice stream margin migration, The Cryosphere, 12, 2545–2568, https://doi.org/10.5194/tc-12-2545-2018, 2018.

Hewitt, I. J.: Modelling distributed and channelized subglacial drainage: the spacing of channels, Journal of Glaciology, 57, 302–314, https://doi.org/10.3189/002214311796405951, 2011.

Hindmarsh, R. C. A.: An observationally validated theory of viscous flow dynamics at the ice-shelf calving front, Journal of Glaciology, 58, 375–387, https://doi.org/10.3189/2012JoG11J206, 2012.

Hulbe, C. and Fahnestock, M.: Century-scale discharge stagnation and reactivation of the Ross ice streams, West Antarctica, Journal of Geophysical Research, 112, F03S27, https://doi.org/10.1029/2006JF000603, 2007.

Joughin, I., Tulaczyk, S., Bindschadler, R., and Price, S. F.: Changes in west Antarctic ice stream velocities: Observation and analysis, Journal of Geophysical Research, 107, 2289, doi:10.1029/2001JB001 029, 2002.

Joughin, I., Smith, B. E., and Schoof, C. G.: Regularized Coulomb Friction Laws for Ice Sheet Sliding: Application to Pine Island Glacier, Antarctica, Geophysical Research Letters, 46, 4764–4771, https://doi.org/10.1029/2019GL082526, 2019.

Kamb, B., Raymond, C., Harrison, W., Engelhardt, H., Echelmeyer, K., Humphrey, N., Brugman, M., and Pfeffer, T.: Glacier surge mechanism: 1982-1983 surge of Variegated Glacier, Alaska, Science, 227, 469–479, 1985.

Kazmierczak, E., Sun, S., Coulon, V., and Pattyn, F.: Subglacial hydrology modulates basal sliding response of the Antarctic ice sheet to climate forcing, The Cryosphere, 16, 4537–4552, https://doi.org/10.5194/tc-16-4537-2022, 2022.

Kazmierczak, E., Gregov, T., Coulon, V., and Pattyn, F.: A fast and unified subglacial hydrological model applied to Thwaites Glacier, Antarctica, EGUsphere, 2024, 1–36, 2024.

Kulessa, B., Hubbard, B., Williamson, M., and Brown, G. H.: Hydrogeological analysis of slug tests in glacier boreholes, Journal of Glaciology, 51, 269–280, https://doi.org/10.3189/172756505781829458, 2005.

Kyrke-Smith, T. M., Katz, R. F., and Fowler, A. C.: Subglacial hydrology and the formation of ice streams, Proceedings of the Royal Society A: Mathematical, Physical and Engineering Science, 470, 20130 494, https://doi.org/10.1098/rspa.2013.0494, 2014.

Kyrke-Smith, T. M., Katz, R. F., and Fowler, A. C.: Subglacial hydrology as a control on emergence, scale, and spacing of ice streams, Journal of Geophysical Research, 120, 1501–1514, https://doi.org/10.1002/2015JF003505, 2015.

MacAyeal, D. R.: Large-scale ice flow over a viscous basal sediment - Theory and application to ice stream B, Antarctica, Journal of Geophysical Research, 94, 4071–4087, https://doi.org/10.1029/JB094iB04p04071, 1989.

MacAyeal, D. R.: Binge/purge oscillations of the Laurentide Ice Sheet as a cause of the North Atlantic's Heinrich events, Paleoceanography,, 8, 775–784, doi:10.1029/93PA02 200, 1993.

https://doi.org/10.5194/egusphere-2025-204
Preprint. Discussion started: 21 February 2025

Mantelli, E. and Schoof, C.: Ice sheet flow with thermally activated sliding. Part 2: the stability of subtemperate regions, Proceedings of the Royal Society A, 475, 20190 411, https://doi.org/10.1098/rspa.2019.0411, 2019.

Mantelli, E., Haseloff, M., and Schoof, C.: Ice sheet flow with thermally activated sliding. Part 1: the role of advection, Proceedings of the Royal Society A, 475, 20190 410, https://doi.org/10.1098/rspa.2019.0410, 2019.

Minchew, B. M. and Meyer, C. R.: Dilation of subglacial sediment governs incipient surge motion in glaciers with deformable beds, Proceedings of the Royal Society A: Mathematical, Physical and Engineering Sciences, 476, 20200 033, https://doi.org/10.1098/rspa.2020.0033, 2020.

Murray, T., Strozzi, T., Luckman, A., Jiskoot, H., and Christakos, P.: Is there a single surge mechanism? Contrasts in dynamics between glacier surges in Svalbard and other regions, Journal of Geophysical Research: Solid Earth, 108, https://doi.org/https://doi.org/10.1029/2002JB001906, 2003.

Ng, F. S. L.: Coupled ice–till deformation near subglacial channels and cavities, Journal of Glaciology, 46, 580–598, https://doi.org/10.3189/172756500781832756, 2000.

Nick, F. M., Vieli, A., Howat, I. M., and Joughin, I.: Large-scale changes in Greenland outlet glacier dynamics triggered at the terminus, Nature Geoscience, 2, 110–114, 2009.

Pattyn, F.: Antarctic subglacial conditions inferred from a hybrid ice sheet/ice stream model, Earth and Planetary Science Letters, 295, 451–461, https://doi.org/10.1016/j.epsl.2010.04.025, 2010.

Payne, A. J. and Dongelmans, P. W.: Self-organization in the thermomechanical flow of ice sheets, Journal of Geophysical Research, 102, 12 219–12 234, doi:10.1029/97JB00 513, 1997.

Pegler, S. S.: The dynamics of confined extensional flows, Journal of Fluid Mechanics, 804, 24–57, 2016.

Peters, L. E., Anandakrishnan, S., Alley, R. B., Winberry, J. P., Voigt, D. E., Smith, A. M., and Morse, D. L.: Subglacial sediments as a control on the onset and location of two Siple Coast ice streams, West Antarctica, Journal of Geophysical Research, 111, B01 302, doi:10.1029/2005JB003 766, https://doi.org/10.1029/2005JB003766, 2006.

Raymond, C. F.: Energy balance of ice streams, Journal of Glaciology, 46, 665–674, https://doi.org/10.3189/172756500781832701, 2000.

Rempel, A. W.: A theory for ice-till interactions and sediment entrainment beneath glaciers, Journal of Geophysical Research (Earth Surface), 113, F01013, https://doi.org/10.1029/2007JF000870, 2008.

Rempel, A. W.: Effective stress profiles and seepage flows beneath glaciers and ice sheets, Journal of Glaciology, 55, 431–443, https://doi.org/10.3189/002214309788816713, 2009.

Retzlaff, R. and Bentley, C. R.: Timing of stagnation of Ice Stream C, West Antarctica, from short-pulse radar studies of buried surface crevasses, Journal of Glaciology, 39, 553–561, https://doi.org/10.3189/S0022143000016440, 1993.

Rignot, E., Mouginot, J., and Scheuchl, B.: Ice Flow of the Antarctic Ice Sheet, Science, 333, 1427–1430, https://doi.org/10.1126/science.1208336, 2011.

Rignot, E., Mouginot, J., Scheuchl, B., Van Den Broeke, M., Van Wessem, M. J., and Morlighem, M.: Four decades of Antarctic Ice Sheet mass balance from 1979–2017, Proceedings of the National Academy of Sciences, 116, 1095–1103, https://doi.org/10.1073/pnas.1812883116, 2019.

Rignot, E., Mouginot, J., Scheuchl, B., and Jeong, S.: Changes in Antarctic Ice Sheet Motion Derived From Satellite Radar Interferometry Between 1995 and 2022, Geophysical Research Letters, 49, e2022GL100 141, https://doi.org/10.1029/2022GL100141, 2022.

Robel, A., Schoof, C., and Tziperman, E.: Rapid grounding line migration induced by internal ice stream variability, Journal of Geophysical Research, 119, 2430–2447, doi:10.1002/2014JF003 251, 2014.

https://doi.org/10.5194/egusphere-2025-204
Preprint. Discussion started: 21 February 2025

Robel, A. A., DeGiuli, E., Schoof, C., and Tziperman, E.: Dynamics of ice stream temporal variability: Modes, scales, and hysteresis, Journal of Geophysical Research, 118, 925–936, https://doi.org/10.1002/jgrf.20072, 2013.

Röthlisberger, H.: Water pressure in subglacial channels, Journal of Glaciology, 11, 177–203, https://doi.org/10.3189/S0022143000022188, 1972.

Sayag, R. and Tziperman, E.: Spontaneous generation of pure ice streams via flow instability: Role of longitudinal shear stresses and subglacial till, Journal of Geophysical Research, 113, B05 411, https://doi.org/10.1029/2007JB005228, 2008.

Schoof, C.: Marine ice-sheet dynamics. Part 1. The case of rapid sliding, Journal of Fluid Mechanics, 573, 27–55, https://doi.org/10.1017/S0022112006003570, 2007a.

Schoof, C.: Ice sheet grounding line dynamics: Steady states, stability, and hysteresis, Journal of Geophysical Research, 112, https://doi.org/10.1029/2006JF000664, 2007b.

Schoof, C.: Ice-sheet acceleration driven by melt supply variability, Nature, 468, 803–806, https://doi.org/10.1038/nature09618, 2010.

Schoof, C.: Marine ice sheet stability, Journal of Fluid Mechanics, 698, 62–72, https://doi.org/10.1017/jfm.2012.43, 2012.

Schoof, C. and Mantelli, E.: The role of sliding in ice stream formation, Proceedings of the Royal Society A, 477, 20200 870, https://doi.org/10.1098/rspa.2020.0870, 2021.

Sergienko, O. and Haseloff, M.: 'Stable' and 'unstable' are not useful descriptions of marine ice sheets in the Earth's climate system, Journal of Glaciology, p. 1–17, https://doi.org/10.1017/jog.2023.40, 2023.

Sergienko, O. and Wingham, D.: Grounding line stability in a regime of low driving and basal stresses, Journal of Glaciology, 65, 833–849, https://doi.org/10.1017/jog.2019.53, 2019.

Sergienko, O. and Wingham, D. J.: Diverse behaviors of marine ice sheets in response to temporal variability of the atmospheric and basal conditions, Journal of Glaciology, pp. 1–12, 2024.

Sevestre, H., Benn, D. I., Luckman, A., Nuth, C., Kohler, J., Lindbäck, K., and Pettersson, R.: Tidewater glacier surges initiated at the terminus, Journal of Geophysical Research: Earth Surface, 123, 1035–1051, https://doi.org/10.1029/2017JF004358, 2018.

Sommers, A., Rajaram, H., and Morlighem, M.: SHAKTI: Subglacial Hydrology and Kinetic, Transient Interactions v1.0, Geoscientific Model Development, 11, 2955–2974, https://doi.org/10.5194/gmd-11-2955-2018, 2018.

Stephenson, S. N. and Bindschadler, R. A.: Observed velocity fluctuations on a major Antarctic ice stream, Nature, 334, 695–697, https://doi.org/10.1038/334695a0, 1988.

Suckale, J., Platt, J. D., Perol, T., and Rice, J. R.: Deformation-induced melting in the margins of the West Antarctic ice streams, Journal of Geophysical Research, 119, 1004–1025, https://doi.org/10.1002/2013JF003008, 2014.

Terleth, Y., Bartholomaus, T. C., Enderlin, E., Mikesell, T. D., and Liu, J.: Glacier Surges and Seasonal Speedups Integrated Into a Single, Enthalpy-Based Model Framework, Geophysical Research Letters, 51, e2024GL112 514, https://doi.org/10.1029/2024GL112514, 2024.

Tsai, V. C., Stewart, A. L., and Thompson, A. F.: Marine ice-sheet profiles and stability under Coulomb basal conditions, Journal of Glaciology, 61, 205–215, 2015.

Tulaczyk, S., Kamb, W. B., and Engelhardt, H. F.: Basal mechanics of Ice Stream B, West Antarctica I. Till mechanics, Journal of Geophysical Research, 105, 463–482, https://doi.org/10.1029/1999JB900329, 2000a.

Tulaczyk, S., Kamb, W. B., and Engelhardt, H. F.: Basal mechanics of Ice Stream B, West Antarctica II. Plastic-undrained-bed-model, Journal of Geophysical Research, 105, 463–482, https://doi.org/10.1029/1999JB900329, 2000b.

Walder, J. S. and Fowler, A.: Channelized subglacial drainage over a deformable bed, Journal of Glaciology, 40, 3–15, https://doi.org/10.3189/S0022143000003750, 1994.

https://doi.org/10.5194/egusphere-2025-204
Preprint. Discussion started: 21 February 2025

Warburton, K., Hewitt, D., and Neufeld, J.: Tidal grounding-line migration modulated by subglacial hydrology, Geophysical Research Letters, 47, e2020GL089 088, https://doi.org/10.1029/2020GL089088, 2020.

Warburton, K. L. P., Hewitt, D. R., and Neufeld, J. A.: Shear dilation of subglacial till results in time-dependent sliding laws, Proceedings of the Royal Society A: Mathematical, Physical and Engineering Sciences, 479, 20220 536, https://doi.org/10.1098/rspa.2022.0536, 2023.

Weertman, J.: Stability of the junction of an ice sheet and an ice shelf, Journal of Glaciology, 13, 3–11, 1974.

Zoet, L. K. and Iverson, N. R.: A slip law for glaciers on deformable beds, Science, 368, 76–78, https://doi.org/10.1126/science.aaz1183, 2020.